Near-field analysis and field transformation applied to a parabolic profile at 5 GHz

S. Peña-Ruiz[a], J. Sosa-Pedroza[a], F. Martínez-Zúñiga[a],

A. Rodríguez-Sánchez[b], E. Garduño-Nolasco[a], and M. Enciso-Aguilar[a]

[a]Instituto Politécnico Nacional, Escuela Superior de Ingeniería Mecánica y Eléctrica.
UPALM Edif. Z-4, Tercer piso, C.P. 07738 Ciudad de México.
[b]Universidad de Quintana Roo Campus Chetumal.
Boulevard Bahía, Esq. Ignacio Comonfort S/N Edif. L, Col. Del Bosque, 77019.
e-mail: srgpr13@gmail.com

We propose a method of near-field analysis and field transformation that is applied to a 1.5 m diameter parabolic reflector at a frequency of 5 GHz. An antenna of such dimensions requires at least a 75 m region to obtain its radiation pattern, and this represents a problem, here arises the necessity to make field transformations like the one presented in this work. Near field is modeled by means of Finite Difference Time Domain Method (FDTD) and current distribution is obtained using the discrete Pocklington equation. Radiation pattern is calculated applying the array factor for parabolic profiles. Results are compared with those obtained by CST Microwave Studio with a very good agreement.

Keywords: Arrays; FDTD; Fraunhofer; modeling; parabolic profile; Rayleigh.

Proponemos un método para el análisis en campo cercano y transformación de campo, que es aplicado a un reflector parabólico de 1.5 m de diámetro, a una frecuencia de 5 GHz, una antena de tales dimensiones requiere una región de al menos 75 m para obtener su diagrama de radiación, lo cual representa un problema, aquí es donde surge la necesidad de realizar transformaciones de campo como la presentada en este artículo. El campo cercano es modelado mediante el método de Diferencias Finitas en el Dominio del Tiempo (MDFDT) y la distribución de corriente es obtenida usando la ecuación discreta de Pocklington. El diagrama de radiación es calculado aplicando el factor de arreglo para perfiles parabólicos. Nuestros resultados del análisis en campo cercano y transformación de campo, son comparados contra el modelado de la estructura en CST Microwave Studio, encontrando muy buenas coincidencias entre ambos métodos.

Descriptores: Arreglos; MDFDT; Fraunhofer; modelado; perfil parabólico; Rayleigh.

PACS: 03.50.De; 02.70.Bf; 41.20.Jb; 07.05.Tp; 01.50.H-   DOI: https://doi.org/10.31349/RevMexFis.65.268

1. Introduction

When a radiated field is distributed in space, there are three regions that identify the process [1]: Rayleigh region, Fresnel region and Fraunhofer region; Rayleigh region refers to the individual point field, which means that the radiation generated at each point of the structure has not been mixed with the other. In Fresnel region, the generated individual fields begin to interact with each other, but their phase differences are significant, so the radiation pattern does not have the shape that must adopt in far-field. In Fraunhofer region, fields are added almost in phase and as they move away from the source, the differences begin to be further reduced, so this region is referred as the far-field region. Figure 1 describes the three regions of the field distribution process in space. Table I shows conditions to determine the field region distances, where D is the antenna diameter, R_1 and R_2 are Rayleigh and Fresnel regions and λ is the wavelength [2].

According with Fig. 1 and Table I, the minimum distance to obtain the far-field of a 1.5 m diameter structure, working at 5 GHz, is at least 75 m, which represents a problem if we try to measure far-field inside a controlled environment (as in an anechoic chamber, making nearly unmanageable to address the problem). Our method proposes to perform a field
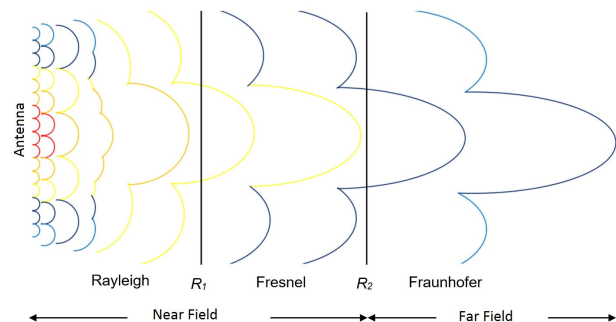

FIGURA 1. Field distribution regions.

TABLE I. Field regions distances.

Antenna dimension	Rayleigh region	Fresnel Region	Fraunhofer region
$D \gg \lambda$	$R_1 < \lambda/2\pi$	$\frac{\lambda}{2\pi} < R_2 < \frac{2D^2}{\lambda}$	$R_2 > \frac{2D^2}{\lambda}$

modeling at the Rayleigh region, define virtual point currents over the surface through discrete Pocklington equation, and then obtain far-field using array theory; essentially a near-field to far-field transformation is carried out. Comparing with commercial software, we reduce computational re-

sources and the proposed method has been used to transform near-field into far-field from real measurements [1].

The method requires knowing the electric field near to reflector surface; this data can be obtained from measurements as [3-6] or by field modeling in the Rayleigh region as in [7], for this purpose, we implement a model based on FDTD method in order to obtain the magnitude and phase of field in a small region, near to the reflector surface. Descriptions of FDTD, discrete Pocklington equation and parabolic array factor (PAF) are presented in following Subsecs. 1.1 and 1.2.

1.1. Finite difference time domain method (FDTD)

The FDTD method allows analyzing the effects of electromagnetic propagation, transforming the differential Maxwell equations into finite difference equations that can be handled by computers [8,9]. FDTD solution involves: establish the analysis region and divide it into cells where Maxwell's equations are approximated by equations in finite differences, considering all materials within the region, using their electric and magnetic characteristics given by their permittivity (ε), permeability (μ) and conductivity (σ); finally the iterative computing solution gives the point field over the region.

Modeled parabolic profile was performed in two dimensions, then propagation is restricted to the XY plane. We choose TM mode considering E_z field as the only transversal component in the XY propagating plane, therefore $E_x = E_y = Hz = 0$. FDTD requires that the analysis region be surrounded by a free reflection computational boundary; we choose Perfectly Matched Layer model (PML) for our application as in [9,10]. Equations (1-4) show the present field components.

$$Ezx_{(i,j)} = \frac{a}{b}Ezx_{(i,j)} + \frac{\Delta t}{\varepsilon b}\left[\frac{Hy_{(i,j)} - Hy_{(i-1,j)}}{\Delta x}\right] \quad (1)$$

$$Ezy_{(i,j)} = \frac{a}{b}Ezy_{(i,j)} - \frac{\Delta t}{\varepsilon b}\left[\frac{Hx_{(i,j)} - Hx_{(i,j-1)}}{\Delta y}\right] \quad (2)$$

$$Hx_{(i,j)} = \frac{c}{d}Hx_{(i,j)} - \frac{\Delta t}{\mu d}\left[\frac{(Ezx + Ezy)_{(i.j+1)}}{\Delta y}\right.$$
$$\left. - \frac{(Ezx + Ezy)_{(i,j)}}{\Delta y}\right] \quad (3)$$

$$Hy_{(i,j)} = \frac{c}{d}Hy_{(i,j)} + \frac{\Delta t}{\mu d}\left[\frac{(Ezx + Ezy)_{(i+1,j)}}{\Delta x}\right.$$
$$\left. - \frac{(Ezx + Ezy)_{(i,j)}}{\Delta x}\right] \quad (4)$$

Where:

$$a = \left(1 - \frac{\sigma\Delta t}{2\varepsilon}\right), \quad b = \left(1 + \frac{\sigma\Delta t}{2\varepsilon}\right),$$

$$c = \left(1 - \frac{\sigma * \Delta t}{2\mu}\right), \quad d = \left(1 + \frac{\sigma * \Delta t}{2\mu}\right),$$

As a primary source we use a standard WR187 waveguide with dimensions of 0.1×0.02215 m working at 5 GHz; as the experiment was performed in 2D, field distribution is given by Eq. (5), with $i = j = 0$ at the origin and E_0 constant.

$$E^n_{z(i,j)} = E_0 \sin(2\pi f n\Delta t) \quad (5)$$

1.2. Discrete Pocklington equation and parabolic array factor

The method considers that the generalized Pocklington equation [11] is valid not only on the antenna surface, but also outside very near to it, as near as the Rayleigh region defines it. Hence, it is possible to perform a field modeling by FDTD or by measurement as in [1] to acquire field points near the structure.

The current can be determined by transforming the generalized Pocklington in a discrete form as Eq. (6) calculating virtual currents I_n along the structure.

$$E^i_m = -\frac{1}{j\omega\varepsilon}\sum_{n=1}^{N}\left[R^2(k^2R^2 - 1 - jkR)S_m \cdot s'_n\right.$$
$$\left. + (3 + 3jkR - k^2R^2)(R \cdot S_m)(R \cdot s'_n)\right]\frac{e^{-jkR}}{4\pi R^5}I_n. \quad (6)$$

Where:

$$R_{mn} = |r - r'|$$
$$= \sqrt{[x(s) - x'(s')]^2 + [y(s) - y'(s')]^2 + [z(s) - z'(s')]^2}$$

k = Wavenumber

Solving Eq. (6) by the structure geometry, it can be constructed a matrix as (7), where Z_{MN} represent impedances, I_N represents a virtual current to be calculated and EM represents the modeled electric field. The matrix is solved by multiplying the electric field vector, obtained by the FDTD modeling, by the inverse of the impedance matrix, so vector current is obtained.
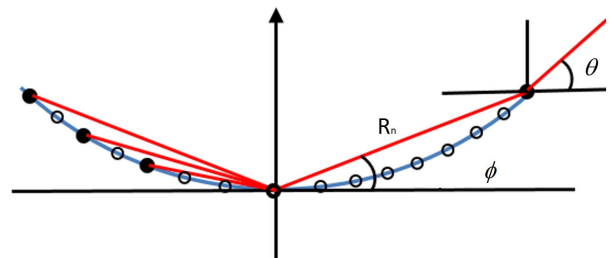

FIGURE 2. Current in a parabolic profile.

$$\begin{bmatrix} Z_{11} & \cdots & Z_{1N} \\ \vdots & \ddots & \vdots \\ Z_{M1} & \cdots & Z_{MN} \end{bmatrix} \begin{bmatrix} I_1 \\ \vdots \\ I_N \end{bmatrix} = \begin{bmatrix} E_1 \\ \vdots \\ E_M \end{bmatrix} \quad (7)$$

Finally, far-field is calculated using the array theory [12,13] under the assumption that calculated point currents I_N in (7), represent an array of specific elements that generate the far-field as is shown in Fig. 2. Field radiated by a parabolic array of point sources is given by (8):

$$PAF(\theta) = E_0 \sum_{n=1}^{N} |I_N| e^{j(kR_n \cos(\theta - \phi) + \alpha_n)} \quad (8)$$

In (8) E_0 represents the reference field of the array point sources with unitary magnitude; the sum of the individual fields from each point antenna considers the phase current α_n, due the distance and the position of each current point R_n defined by ϕ while θ represents the angle between each point and the far-field position, Fig. 2 describes Eq. (8).

2. Near-field analysis and far-field transformation

Table II shows the modeling parameters, where physical dimensions are defined in meters and cells, in order to apply our computational technique based on Pocklington equation and FDTD.

Calculus region dimensions are 1.5×2.25 m corresponding to 500×750 cells, considering the size of each cell as $\lambda/20$, even several authors define $\lambda/10$ is an acceptable size [9]. Our results are compared with those of commercially available software CST, using same parameters for both experiments. Figure 3 shows the calculus region and electric field distribution for both computational methods. To have a better view of the parabolic profile, Fig. 3 (a) is shown in a smaller area defined by (90:335,95:645), where reflector
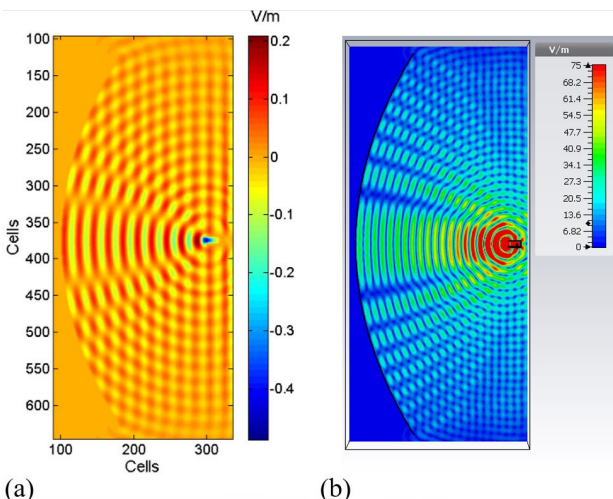

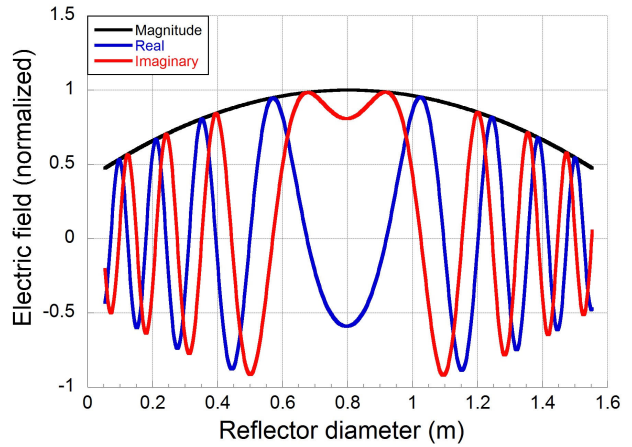FIGURE 3. Near-field modeling at 5 GHz, a) FDTD and b) CST.

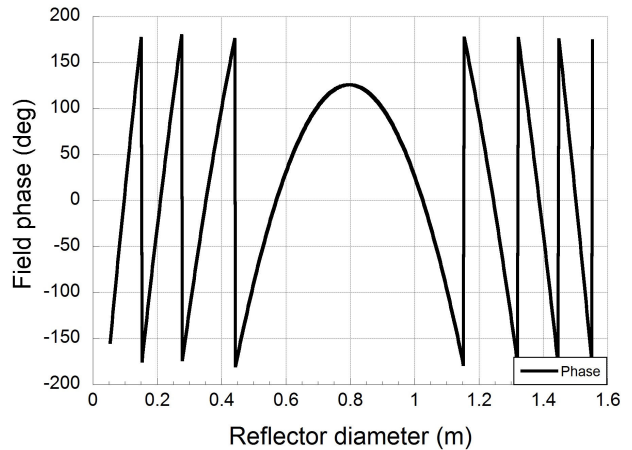FIGURE 4. Superficial electric field distribution.

FIGURE 5. Field distribution phase.

TABLE II. Modeling parameters at 5 GHz.

Units	Cells	m
wavelength	λ	0.06
Cell	$\lambda/20$	0.003
Calculus region	500×750	1.5×2.25
Plate diameter	500	1.5
Vertex - focus	200	0.6
Vertex - edge	77	0.23
height (feeder)	7	0.02215
depth (feeder)	33	0.1
PML	24	0.07

vertex is located at (100,375) and its focus at (300,375). Figure 3 displays both incident and reflected fields, which visual comparison with CST shows a very good concordance.

The electric field vector E_M in Rayleigh region required in (6), is defined using field samples from 500 points in the FDTD matrix at 0.003 m, one cell away from reflector surface along the parabolic profile. Figure 4 shows E_M vector
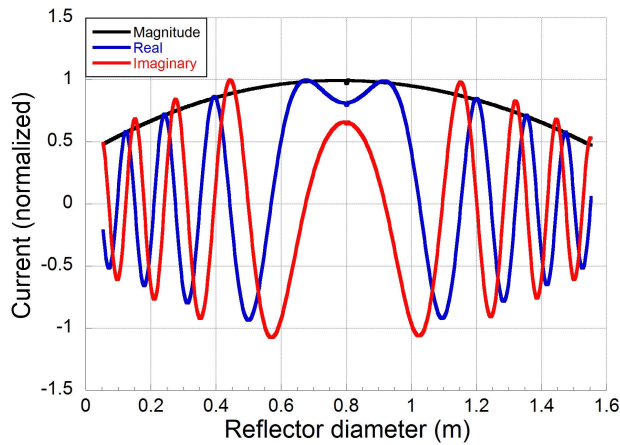
FIGURE 6. Superficial current distribution.

in magnitude, real and imaginary parts. Field phase is shown in Fig. 5, and is obtained using distances from reflector surface to its focus, for each field point using parabola equation [14].

Next step in the methodology is to apply Eqs. (6) and (7) to obtain current along the reflector surface. Equation (6) requires the use of parabolic geometry for distance R_{mn} and vectors s_m and s_n, that is, distances between each point of the reflector axis and each current point [7].

Finally, the field distribution is transformed in virtual point currents along the plate surface that will be applied in the array factor equation for the parabolic profile (8). Figure 6, shows the magnitude, real and imaginary normalized parts for current distribution I_N. We can notice a similar behavior with electric field displayed on Fig. 4, including the 180° phase change of imaginary part due the reflection. Figure 7 shows the calculated phase for each current point.

Once field distribution is transformed into virtual currents along the parabolic profile, magnitude and phase values are used in the parabolic array factor Eq. (8) to get the far-field pattern shown in Fig. 8. As it is shown, radiation pattern has a main lobe width of 2.5° which is consistent with the theory of parabolic reflectors [15], also the nearest sidelobes are ob-
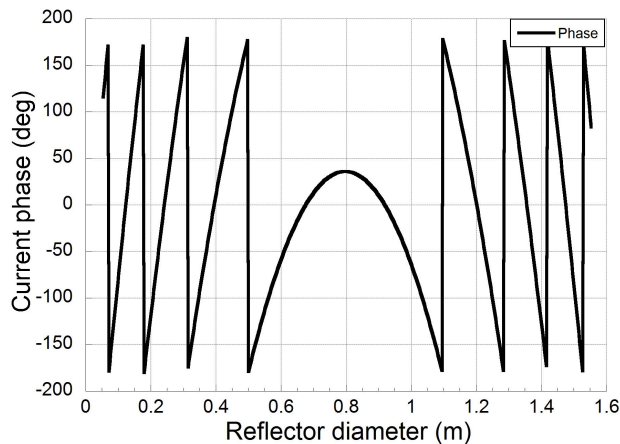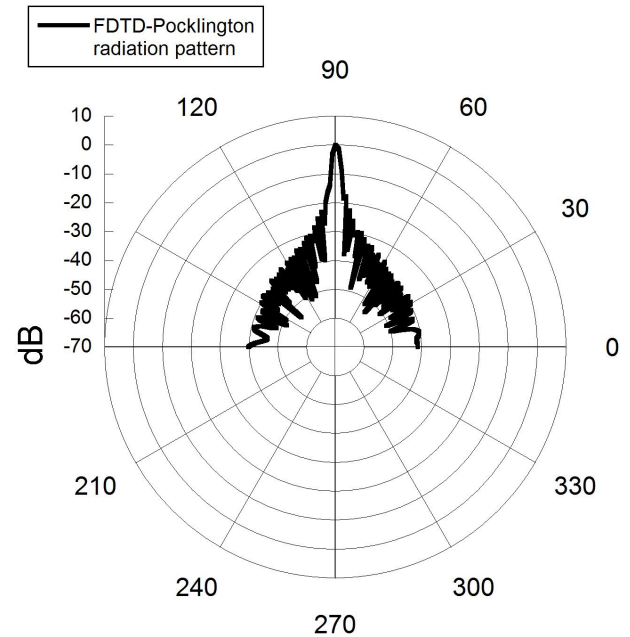

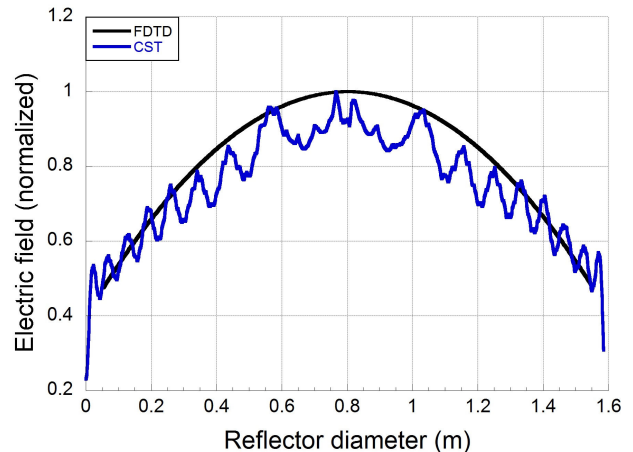FIGURE 8. Reflector field pattern at 5 GHz.

FIGURE 9. Magnitude Electric field comparison between FDTD and CST.

served at −17 dB, other lobes have amplitudes between −20 dB and −55 dB.

3. Comparison

In previous work [7,16], calculated radiation pattern was compared versus a measured radiation pattern however, actual analysis allows us to observe and compare electric field behavior with those calculated in CST to show its viability.

Figure 9 shows a comparison between near-field behavior for both simulations (FDTD and CST) in magnitude. Figures 10 and 11 show an excellent agreement of the near-field in real and imaginary parts; finally, near-field phase is shown in Fig. 12, as seen there is a clear similarity between FDTD and
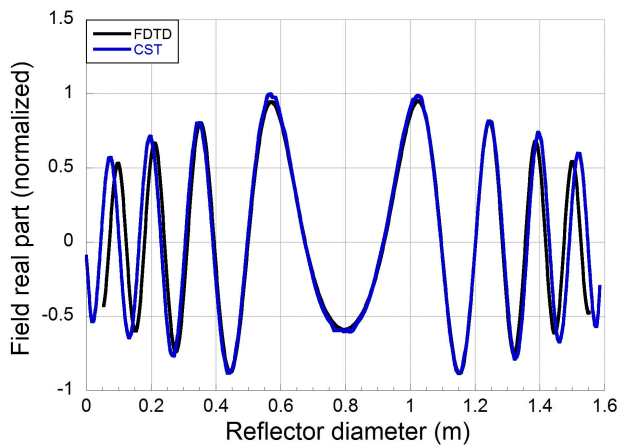

FIGURE 7. Current phase.

FIGURE 10. Electric field real part comparison between FDTD and CST.
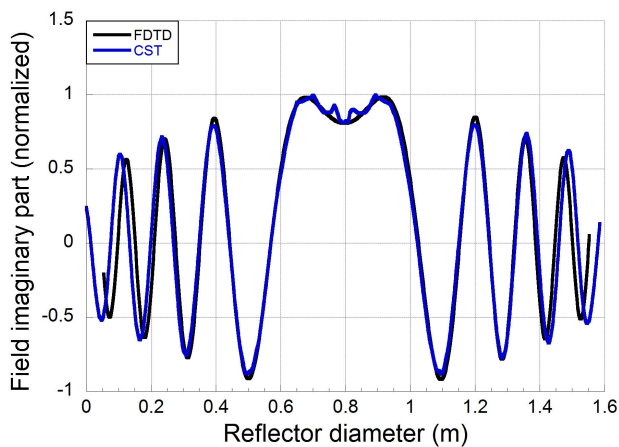

FIGURE 11. Electric field imaginary part comparison between FDTD and CST.
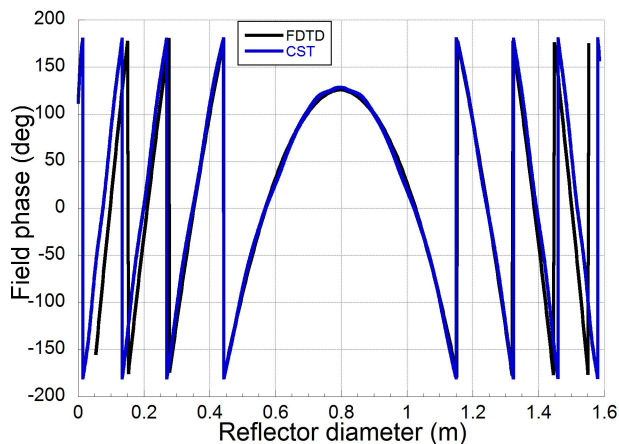

FIGURE 12. Electric field phase comparison between FDTD and CST.

CST curves, specially real and imaginary parts with small differences at the beginning and at end of curves.

Radiation patterns comparison is shown in Fig. 13, black curve represents the pattern of our method and blue curve is
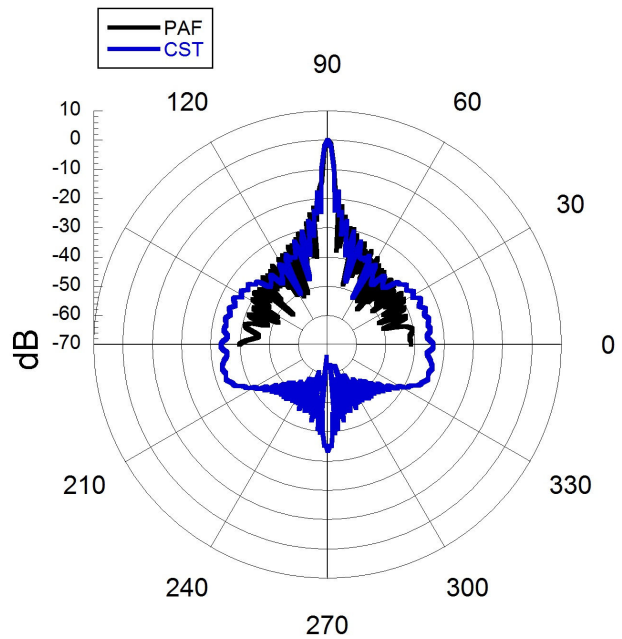

FIGURE 13. Reflector field pattern comparison at 5 GHz.

the CST pattern. Similarity between both curves is evident; it can be seen that the main lobe width is about 2.5° for both patterns and small differences of 5 dB at the edges (0° to 30° and 150° to 180°).

4. Conclusions

We presented a method to transform near-field (Rayleigh region) into far-field, without performing simulation in large computational regions, then reducing computing resources. Even we define the field in the Rayleigh region using the FDTD Method, an alternative proposed as future work is to measure the field near the reflector surface and obtain far-field with Pocklington equation and Array Theory. In addition, our method can be applied to other antenna geometries as lineal radiators or even linear arrays or some other type of reflectors.

Comparison between our methodology (FDTD-Pocklington-PAF) and commercial software shows that results are very similar not only for radiation pattern, but also for near-field behavior.

Acknowledgments

1. J. Sosa-Pedroza, L. Carrion-Rivera, F. Martínez-Zúñiga and S. Peña-Ruiz, *Una Propuesta para Transformar Mediciones de Campo Cercano en Campo Lejano*. Simposio de Metrología CENAM, México (2014).

2. Y. Huang, K, Boyle, *Antennas from Theory to Practice*. (John Wiley. UK, 2008), p. 109-112.

3. M. Sierra-Castañer, S. Burgos. *Fresnel Zone to Far Field Algorithm for Rapid Array Antenna Measurements*. IEEE EUCAP (2011).

4. R. Cornelius, T. Salmerón-Ruiz, F. Saccardi, L. Foged, D. Heberling, M. Sierra-Castañer, *IEEE Antennas and Propagation Magazine* **56** (2014) .

5. F. D'Agostino *et al.*, *IEEE Antennas and Propagation Magazine* **54** (2012).

6. S. Costanzo, G. Di Massa, *Microwave and Optical Technology Letters* **48** (2006).

7. J. Sosa-Pedroza, M. Enciso-Aguilar, S. Peña-Ruiz, A. Rodríguez-Sánchez, and E. Garduño-Nolasco, *Microwave and Optical Technology Letters* **58** (2016).

8. J. Sosa-Pedroza *et al.*, *Approach. Electron. Lett*. **47** (2011) 1308-1309.

9. A. Taflove and S. C. Hagness, *Computational Electrodynamics The Finite-Diference Time-Domine Method*. (Artech House USA 2005) p. 54-75.

10. M. Benavides *et al.*, *Rev. Mex. Fís. E* **57** (2011) 25-31.

11. J. Sosa-Pedroza , V. Barrera-Figueroa and J. López-Bonilla, *Pocklington Equation and the Method of Moments Proc. Pakistan Acad*. (2005).

12. C. A. Balanis, *Antenna Theory Analysis and Design*. 3rd Ed. (John Willey, 2005) p. 284-313.

13. L. Josefsson, P. Persson, *Conformal Array Antenna Theory and Design. IEEE* (Press Series on Electromagnetic Wave Theory. USA, 2006), p. 15-22.

14. Jacob W.M. Baars, *The Paraboloidal Reflector Antenna in Radio Astronomy and Communication*. (Springer Science USA, 2007), p. 14-16.

15. J. D. Kraus, R. J. Marhefka, *Antennas for all Applications*. 3rd Ed. (McGraw Hill. USA, 2002), p. 564-571.

16. J. Sosa, S. Peña, F. Martínez, *Parabolic Reflector Near-field to Far-field Transformation Using FDTDM and Pocklington Equation*. PIERS, (2017).